# Photoinduced Energy Transfer in Associated but Noncovalently Linked Photosynthetic Model Systems

**Jonathan L. Sessler,*,§ Bing Wang,§ and Anthony Harriman*,†**

*Contribution from the Department of Chemistry and Biochemistry and Center for Fast Kinetics Research, University of Texas at Austin, Austin, Texas 78712*

*Received August 5, 1994*[⊗]

**Abstract:** The synthesis and photophysical characterization of nucleobase-substituted porphyrins designed to form rigid hydrogen-bonded ensembles, and to allow for energy transfer within the resulting complexes, is reported. Watson-Crick nucleobase-pairing interactions between guanosine- and cytidine-bearing porphyrins are used to assemble the hydrogen-bonded ensembles. Likewise, zinc(II) and free-base porphyrins are used respectively as the donors and acceptors within these ensembles that, depending on design, contain either two or three total porphyrin subunits within the supramolecular assembly. The association constant for guanosine-to-cytidine association, representing the primary interaction in each donor-acceptor assembly, is *ca.* 22 000 ± 2000 $M^{-1}$ in $CD_2Cl_2$ as determined from $^1H$ NMR titration analyses. Both singlet and triplet energy transfer was observed within the various donor-acceptor assemblies. Whereas the singlet-state energy-transfer dynamics are consistent with a Förster-type process, triplet energy transfer within the same complex is believed to occur through the hydrogen-bonded interface. The presently-described noncovalent approach to donor-acceptor ensemble generation is thus considered to provide a novel and useful approach to modeling aspects of the photon antennae that are part of the natural photosynthetic process.

## Introduction

Solar energy conversion in nature, such as that effected by photosynthetic bacteria, is a process of both great importance and great complexity. It begins with the capture of sunlight by hundreds of chlorophyll arrays and the commensurate funneling of that energy to a reaction center *via* efficient energy migration and transfer.[1] A subsequent series of electron-transfer events within the reaction center complex then produces a long-lived, transmembrane charge-separated state.[2] This charge-separated state, in turn, provides a means of storing energy (as chemical potential) for eventual use in various biochemical reactions.

Understanding the factors that govern the energy- and electron-transfer processes in natural photosynthetic systems is an important prerequisite to the manufacture of, for instance, solar energy conversion devices. Considerable research effort, therefore, has been devoted to the study of these processes, and, in this context, a large number of supramolecular model systems have been prepared.[3-5] Most of these were introduced in an effort to obtain insight into the charge-separating electron-transfer events, as opposed to the initial energy-transfer process. Nonetheless, the models prepared to date have proved to be extremely useful. For example, studies made with many covalently-linked, donor-acceptor model systems[3] have served to reveal the effects of structural factors, such as distance and orientation, as well as parameters associated with the electronic nature of the spacer, overall energetics (*i.e.*, the driving force), temperature, and solvent on the rates of the charge-separation process. Also, recent reports have described the use of noncovalent approaches[4,5] to address biological electron-transfer pathway issues.[4a,5] Interestingly, less attention has been paid to the generation of model systems that might elucidate key mechanistic questions associated with the light-harvesting antennae that are an integral part of photosynthesis.[6] Indeed, to date, there have been only a few relevant reports, and nearly all of these involved covalently-linked tetrapyrrolic dimers and oligomers.[7-9] Unfortunately, this covalent approach is necessarily limited in scope and faces real obstacles when one attempts to construct and characterize higher-order arrays of

§ Department of Chemistry and Biochemistry.

† Center for Fast Kinetics Research.

⊗ Abstract published in *Advance ACS Abstracts,* January 1, 1995.

(1) For reviews see: (a) Robinson, G. W. *Brookhaven Symp. Biol.* **1967**, *19*, 16. (b) Pearlstein, R. H. *New Compr. Biochem.* **1987**, *15*, 299. (c) Fleming, G. R.; Martin, J.-L.; Breton, J. *Nature* **1988**, *333*, 190.

(2) (a) Paddock, M. L.; Rongey, S. H.; Feher, G.; Okamura, M. Y. *Proc. Natl. Acad. Sci. U.S.A.* **1989**, *86*, 6602. (b) Feher, G.; Allen, J. P.; Okamura, M. Y.; Rees, D. C. *Nature* **1989**, *339*, 111.

(3) For reviews of covalently-linked donor-acceptor ET systems, see: (a) Connolly, J. S.; Bolton, J. R. In *Photoinduced Electron Transfer, Part D*; fox, M. A., Chanon, M., Eds.; Elsevier: Amsterdam, 1988; p 303. (b) Wasielewski, M. R. *Chem. Rev.* **1992**, *92*, 435. (c) Dixon, M.; Fajer, J.; Feher, G.; Freed, J. H.; Gamliel, D.; Hoff, A. J.; Levanon, H.; Möbius, K.; Norris, J. R.; Nechushtai, R.; Scherz, A.; Sessler, J. L.; Stehlik, D. H. A. *Isr. J. Chem.* **1992**, *32*, 369.

(4) For noncovalently linked donor-acceptor ET systems, see: (a) Turro, C.; Chang, C. K.; Leroi, G. E.; Cukier, R. I.; Nocera, D. G. *J. Am. Chem. Soc.* **1992**, *114*, 4013. (b) Aoyama, Y.; Asakawa, M.; Matsui, Y.; Ogoshi, H. *J. Am. Chem. Soc.* **1991**, *113*, 6233. (c) Hayashi, T.; Miyahara, T.; Hashizume, N.; Ogoshi, H. *J. Am. Chem. Soc.* **1993**, *115*, 2049. (d) Kuroda, Y.; Ito, M.; Sera, T.; Ogoshi, H. *J. Am. Chem. Soc.* **1993**, *115*, 7003. (e) Collin, J.-P.; Harriman, A.; Heitz, V.; Odobel, F.; Sauvage, J.-P. *J. Am. Chem. Soc.* **1994**, *116*, 5679.

(5) (a) Harriman, A.; Kubo, Y.; Sessler, J. L. *J. Am. Chem. Soc.* **1992**, *114*, 388. (b) Sessler, J. L.; Wang, B.; Harriman, A. *J. Am. Chem. Soc.* **1993**, *115*, 10 418.

(6) Barber, J.; Anderson, B. *Nature* **1994**, *370*, 31 and references therein.

(7) For examples of covalently-linked donor-acceptor systems used to study energy transfer processes, see: (a) Milgrom, L. R. *J. Chem. Soc., Perkin Trans.* **1983**, 2535. (b) Davila, J.; Harriman, A.; Milgrom, L. R. *Chem. Phys. Lett.* **1987**, *136*, 427. (c) Chardon-Nobalt, S.; Sauvage, J.-P.; Mathis, P. *Angew. Chem., Int. Ed. Engl.* **1989**, *28*, 593. (d) Meier, H.; Kobuke, Y.; Kugimiya, S. *J. Chem. Soc., Chem. Commun.* **1989**, 923. (e) Rempel, U.; von Maltzan, B.; von Borczykowski, C. *Chem. Phys. Lett.* **1990**, *169*, 347. (f) Osuka, A.; Maruyama, K.; Yamazaki, I.; Tamai, N. *Chem. Phys. Lett.* **1990**, *165*, 392. (g) Rodriguez, J.; Kirmaier, C.; Johnson, M. R.; Friesner, R. A.; Holten, D.; Sessler, J. L. *J. Am. Chem. Soc.* **1991**, *113*, 1652. (h) Gust, D.; Moore, T. A.; Moore, A. *Acc. Chem. Res.* **1993**, *26*, 198. (i) Gust, D.; Moore, T. A.; Moore, A.; et al. *J. Am. Chem. Soc.* **1993**, *115*, 11 141. (j) Prathapan, S.; Johnson, T. E.; Lindsey, J. S. *J. Am. Chem. Soc.* **1993**, *115*, 7519. (k) Harriman, A.; Capuano, V. L.; Sessler, J. L. *J. Am. Chem. Soc.* **1993**, *115*, 4618. (l) Lin, V. S.-Y.; DiMagno, S. G.; Therien, M. J. *Science* **1994**, *264*, 1105.

(8) (a) Harriman, A.; Magda, D.; Sessler, J. L. *J. Chem. Soc., Chem. Commun.* **1991**, 345. (b) Harriman, A.; Magda, D. J.; Sessler, J. L. *J. Phys. Chem.* **1991**, *95*, 1530.

0002-7863/95/1517-0704$09.00/0 

**Chart 1**

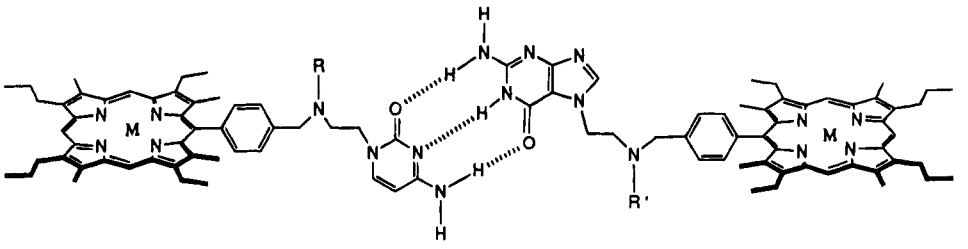

I

R, R' = $-CH_2CH_2OCH_2CH_2OCH_3$ or 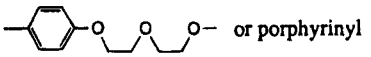 or porphyrinyl

M = Zn or $H_2$

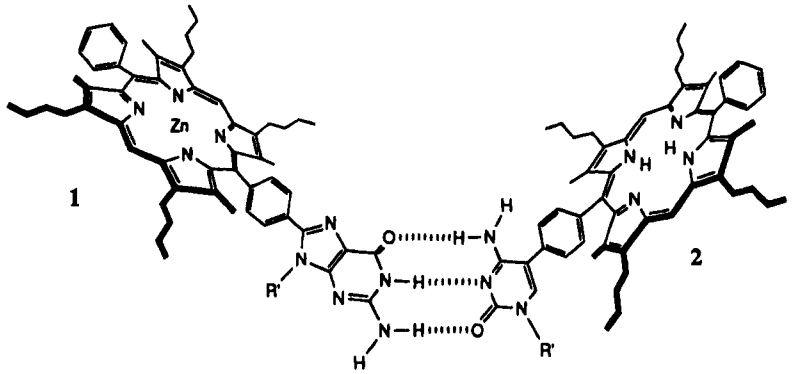

II

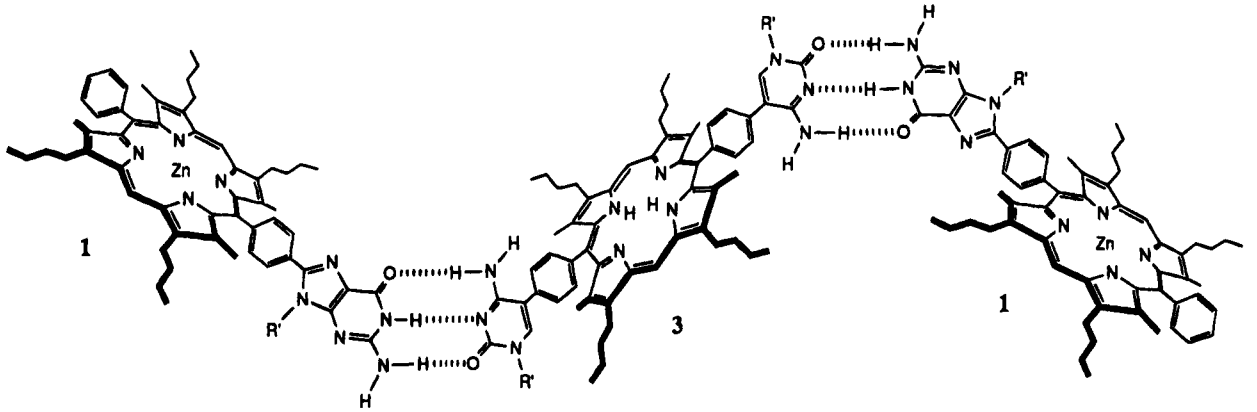

III

R' = 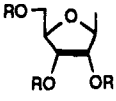 , R = $SiMe_2Bu^t$

chromophores. Thus, model systems that use noncovalent forces as the means of establishing phonon antennae could present considerable advantages.[8,9] They could, in particular, allow for the ordered assembly of chromophoric arrays analogous to those found in photon antennae. More to the point, such an approach would allow the initial preparation of recognition-unit-bearing chromophores that, when allowed to self-assemble as "mix and match" monomeric building blocks, could give rise to an ordered array containing multiple chromophores. This paper is concerned with such a strategy.

Earlier, we established, in the context of reporting the preparation of ensemble **I**, that noncovalently assembled supramolecular complexes could be constructed using Watson–Crick-type nucleic acid base ("nucleobase") pairing interactions between guanine (G) and cytosine (C).[8] In this particular ensemble, which is stabilized by multiple hydrogen-bonding interactions, photoinduced triplet–triplet energy transfer was observed within the hydrogen-bonded complex following illumination. Unfortunately, these first generation systems proved to be very flexible. As a consequence, no singlet–singlet energy transfer was observed. Also, the mechanistic details of the observed energy-transfer process remained indeterminate. Intracomplex diffusional encounter between the donor and acceptor, rather than a through hydrogen bond energy-transfer process, could have been invoked, for instance, to account for the observed triplet–triplet energy transfer.

(9) For examples of other approaches being pursued in the study of noncovalent energy-transfer phenomena, see: (a) Tecilla, P.; Dixon, R. P.; Slobodkin, G.; Alavi, D. S.; Waldeck, D. H.; Hamilton, A. D. *J. Am. Chem. Soc.* **1990**, *112*, 9408. (b) Causgrove, T. P.; Cheng, P.; Brune, D. C.; Blankenship, R. E. *J. Phys. Chem.* **1993**, *97*, 5519. (c) Hildebrandt, P.; Tamiaki, H.; Holzwarth, A. R.; Schaffner, K. *J. Phys. Chem.* **1994**, *98*, 2192.

Given the limitations inherent in ensemble **I**, it was decided that a better defined system would be needed in order to interpret unambiguously the dynamics of energy-transfer processes in this kind of G–C base-pairing derived noncovalent model system. In this paper, we present the syntheses and photophysical characterization of two such rigid, second-generation, model systems. In the first of these, ensemble **II**, a dimeric porphyrin array, the energy donor (namely, a zinc(II) porphyrin) and acceptor (namely, a free-base porphyrin) are connected *via* a phenyl group to guanosine (G) and cytidine (C) recognition units, respectively. The two porphyrins are arranged side-by-side with an interplane angle of *ca.* 90° and with the porphyrin-to-porphyrin center-to-center distance being *ca.* 22.5 Å, as estimated from CPK models. Here, it is important to appreciate that each porphyrin possesses *ca.* 45° of rotational freedom around the carbon–carbon bond connecting the phenyl and nucleobase entities. In the second ensemble, namely **III**, two G–C base-pairing interactions are used to establish a higher-order porphyrinic array wherein two zinc porphyrins and one free-base porphyrin are held together in a trimeric configuration. In both ensembles, protected ribosyl groups are present on the nucleobases for solubility purposes.

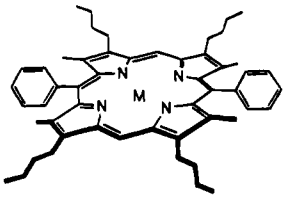

4: M = $H_2$

5: M = Zn

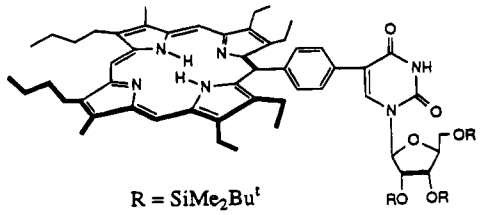

R = $SiMe_2Bu^t$

6

## Results and Discussion

**Synthesis.** The new compounds reported here for the first time (**2** and **3**), or in full detail (**1**),[5b] were prepared from two intermediates, namely, the guanosine- and cytidine-substituted benzaldehydes **11** and **19** (Schemes 1 and 2), using the so-called MacDonald–Chang porphyrin synthesis.[10,11] These crucial intermediates were, in turn, obtained by the application of a versatile carbon–carbon bond formation method, the so-called *Stille* cross-coupling reaction,[12] that involves the Pd-catalyzed coupling between an organostannyl benzaldehyde derivative and a halogenated nucleobase. This chemistry is summarized in Schemes 1 and 2 and explicitly discussed below.

The organostannyl benzaldehyde derivative **9** was prepared in 67% yield from 4-bromobenzaldehyde (**7**) and bis(tributyltin) (**8**) in the presence of $Pd(PPh_3)_4$ using a modification of a known procedure.[13] From this organotin compound and the isobutyryl protected 8-bromoguanosine (**10**), the first key intermediate, namely, the guanosine-substituted benzaldehyde **11**, could be prepared. Specifically, it was synthesized in 70% yield under conditions of $Pd(PPh_3)_4$ mediated coupling (toluene, argon atmosphere, reflux).

Surprisingly, only very low yields of the coupled product were obtained when the same coupling procedure was tried using the organostannyl precursor **9** and a benzoyl-protected 5-bromocytidine derivative **13** as the two reactants. Nonetheless, a successful route to the desired product from this reaction, namely, the cytidine-substituted benzaldehyde **19**, was developed as shown in Scheme 2. In this latter sequence, 4-bromobenzaldehyde was replaced with 4-bromobenzyl alcohol **14** since it was found that a much higher yield could be attained if an aryl organotin precursor, containing one or more electron-donating substituents on the benzene ring, was used. Compound **14** was then allowed to couple with a 5-bromocytidine derivative, such as **13**. Thus, 4-bromobenzyl alcohol **14** was first *O*-protected using a *tert*-butyldimethylsilyl (TBDMS) group to

**Scheme 1**

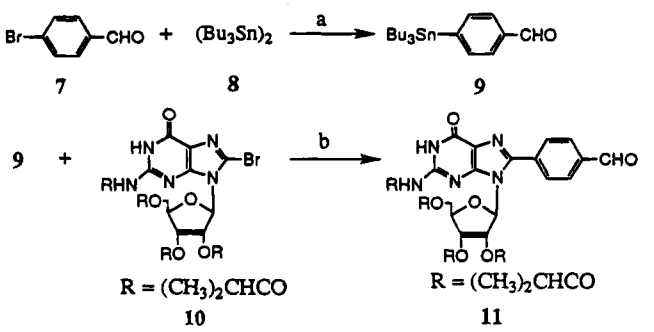

(a) $Pd(PPh_3)_4$, toluene, argon, reflux, 15 h. (b) $Pd(PPh_3)_4$, toluene, argon, reflux, 24 h.

**Scheme 2**

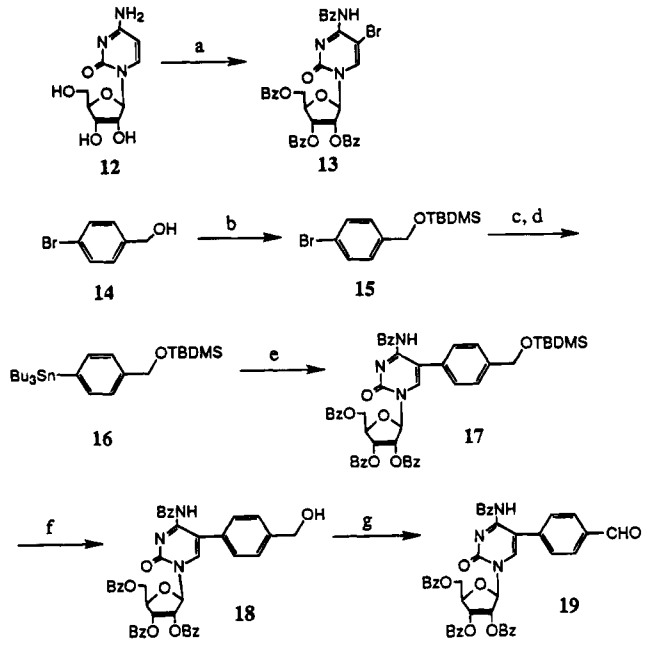

(a) (i) $Br_2$, pyridine, room temperature, 45 min; (ii) BzCl, pyridine, room temperature, 2 h. (b) TBDMS-Cl, imidazole, DMF, room temperature, overnight. (c) *n*-BuLi, THF, −78 °C, 30 min. (d) $Bu_3SnCl$, THF, room temperature, 2 h. (e) **13**, $Pd(PPh_3)_4$, toluene, argon, reflux, 40 h. (f) TBAF, THF, room temperature, 20 h. (g) PDC, $CH_2Cl_2$, room temperature, 3 h.

(9) Arsenault, G. P.; Bullock, E.; MacDonald, S. F. *J. Am. Chem. Soc.* **1960**, *82*, 4384.

(10) Chang, C. K.; Abdalmuhdi, I. *J. Org. Chem.* **1983**, *48*, 5388.

(11) (a) Stille, K. *Angew. Chem., Int. Ed. Engl.* **1986**, *25*, 508 and references therein. (b) Kalinin, V. N. *Synthesis* **1992**, 413 and references therein. (c) Mitchell, T. N. *Synthesis* **1992**, 803 and references therein.

(12) Azizian, H.; Eaborn, C.; Pidcock, A. *J. Organomet. Chem.* **1981**, *215*, 49.

**Scheme 3**

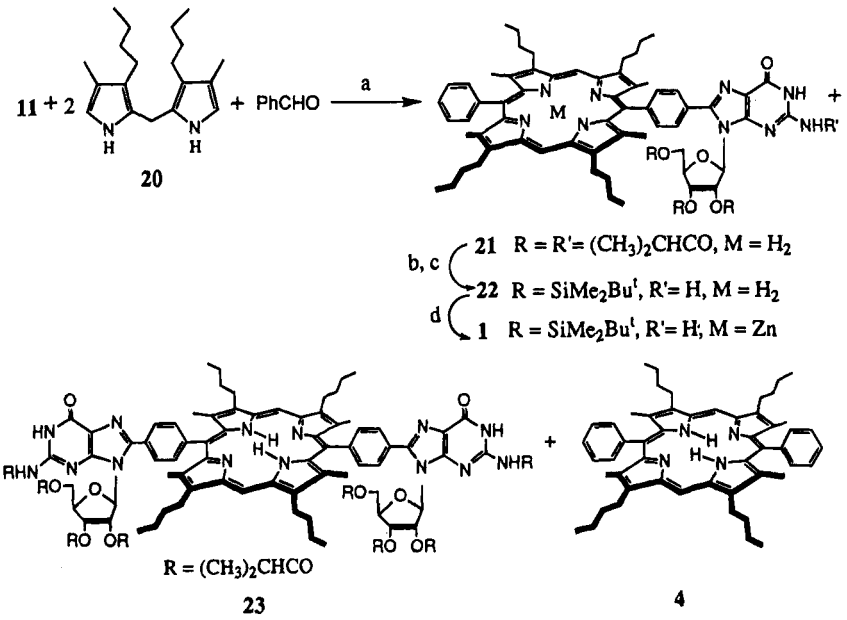


(a) (i) TFA, $CH_2Cl_2$, argon, room temperature, 4 h; (ii) NaOAc, 30 min; (iii) *p*-chloranil, room temperature, 6 h. (b) $NH_3$/MeOH, room temperature, 36 h. (c) TBDMS-Cl, imidazole, DMF, room temperature, overnight. (d) ZnOAc, MeOH, reflux, 30 min.

**Scheme 4**

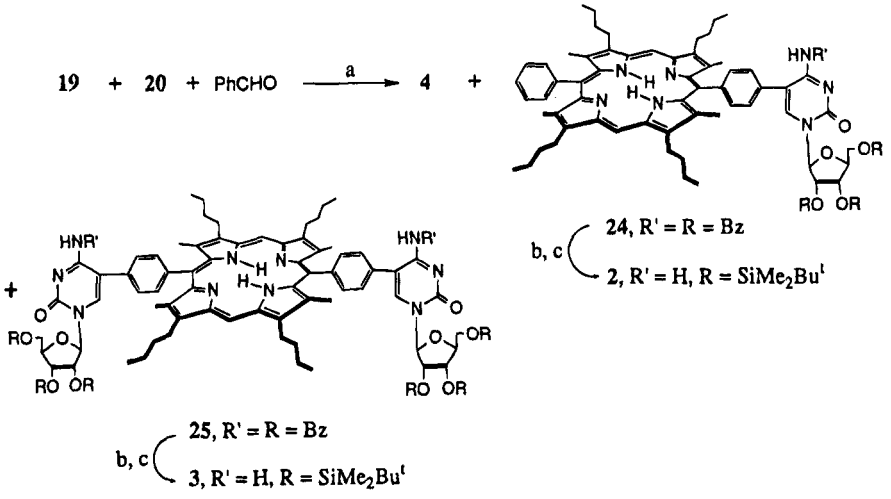


(a) (i) TFA, $CH_2Cl_2$, argon, room temperature, 7 h; (ii) NaOAc, 1 h; (iii) *p*-chloranil, room temperature, overnight. (b) $NH_3$/MeOH, room temperature, 36 h. (c) TBDMS-Cl, imidazole, DMF, room temperature, overnight.

give **15** in excellent yield. Following lithiation–transmetalation exchange (*n*-butyllithium, −78 °C; then $Bu_3SnCl$, room temperature), the masked organotin compound **16** was obtained in 78% yield. With this precursor in hand, the Pd-catalyzed coupling could be carried out with the benzoyl-protected 5-bromocytidine **13** (prepared in 86% yield from cytidine **12** *via* a one-pot reaction procedure). Although the resulting product **17** was difficult to separate from unreacted **13**, it could nonetheless be used in the subsequent steps. Indeed, the ensuing desilylation step (TBAF in THF), carried out using a mixture of **13** and **17**, gave an easily purified product, namely, the cytidine-derived benzyl alcohol **18** in 56% overall yield. This latter intermediate was transformed in good yield to the corresponding aldehyde **19**, using pyridinium dichromate (PDC) at room temperature as the oxidant.

Once in hand, these two key nucleobase-substituted benzaldehyde derivatives were used to prepare a number of nucleic acid functionalized porphyrins. The relevant synthetic chemistry is summarized in Schemes 3 and 4. Thus, Scheme 3 illustrates how masked guanosine porphyrins, such as **21**, were synthesized. Briefly, condensation of the guanosine-substituted benzaldehyde **11** with benzaldehyde and 4,4′-dimethyl-3,3′-dibutyldipyrrylmethane (**20**),[14] under the optimized conditions introduced by Lindsey,[15] gave rise to three porphyrins, namely, the monoguanosine porphyrin **21** (27%), the diguanosine porphyrin **23** (33%), and the corresponding 5,15-diphenylporphyrin **4** (25%). Subsequent deprotection (saturated methanolic ammonia, room temperature) and selective reprotection (TBDMS-Cl, imidazole, DMF) of the monoguanosine porphyrin **21** gave rise to the unmasked guanosine porphyrin **22**. This latter compound (used without further purification) was converted into its corresponding zinc porphyrin **1** in 50% overall yield following column chromatographic purification.

As illustrated in Scheme 4, the same basic method could be

(13) (a) Sessler, J. L.; Johnson, M. R.; Creager, S. E.; Fettinger, J. D.; Ibers, J. A. *J. Am. Chem. Soc.* **1990**, *112*, 9310. (b) Sessler, J. L.; Mozaffari, A.; Johnson, M. R. *Org. Synth.* **1991**, *70*, 68. (c) Barton, D. H.; Zard, S. Z. *J. Chem. Soc., Chem. Commun.* **1985**, 1098.

(14) Lindsey, J. S.; Schreiman, I. C.; Hsu, H. C.; Kearney, P. C.; Marguerettaz, A. M. *J. Org. Chem.* **1987**, *52*, 827.

used to generate a 9:6:3 mixture of porphyrins **4**, **24**, and **25**. In this case, the starting materials were the 5-cytidine-substituted benzaldehyde **19**, benzaldehyde, and the alkylated dipyrrylmethane **20**. Subsequent deprotection and selective reprotection of the two cytidine porphyrins, **24** and **25**, then served to furnish the desired unmasked mono- and dicytidine porphyrins **2** and **3**, respectively.

**Interactions between Guanosine- and Cytidine-Substituted Porphyrins.** A crucial predicate of the current noncovalent approach to photosynthetic modeling is that specific noncovalent interactions between guanosine- and cytosine-bearing donors and acceptors can be used to assemble putative antenna-like ensembles. Thus, these two nucleic acid bases not only provide a means of tethering together the proposed donor and acceptor, they also provide a possible hydrogen-bonded pathway through which (exchange-type) energy transfer might be facilitated. The need to evaluate the magnitude of the associative interaction between cytosine and guanine thus becomes apparent. Of course, for this evaluation to be most informative, it should be done using cytosine and guanine systems that contain the actual donors and acceptors of interest.

It is well known that there are two kinds of noncovalent interactions between nucleobases that are significant in biological systems; namely, $\pi-\pi$ stacking and hydrogen bonding.[16] Hydrogen bonding can be further categorized into the so-called Watson–Crick (three-point hydrogen bonding) and Hoogsteen (two-point hydrogen bonding) base pairing. Stacking interactions are favored in aqueous solution[16] and can be excluded as far as the present aprotic solvent-based studies are concerned. Hoogsteen G–C base pairing can also be ruled out as being important in our ensembles since this kind of interaction requires protonation of the cytosine subunit at its N3 position.[17] Thus the major C–G interaction operative in our systems is considered to be Watson–Crick base pairing.

Quantitative assessment of the strength of the proposed C-to-G hydrogen bonding in our systems came from proton NMR titration analyses. Specifically, addition of increasing quantities of cytidine-bearing porphyrin **2** into a solution of guanosine-appended zinc porphyrin **1** in $CD_2Cl_2$ at 23 °C gave rise to chemical shift changes of the imino proton of the guanosine subunit (N1–H). Analysis of the observed chemical shift change using a standard curve-fitting program[18] (Figure 1) gave an association constant of 22 000 ± 2000 $M^{-1}$ for C-to-G base pairing within this particular ensemble (**II**). Thus the association constant obtained is comparable to those reported previously for other functionalized G–C base pairs under similar experimental conditions.[5b,19]

A closer look at the titration data given in Figure 1 shows that the binding profile reaches a plateau near a 1:1 molar ratio of **1** and **2**. Such a finding is consistent with 1:1 stoichiometric binding between **1** and **2** as would be expected on the basis of simple chemical intuition. It is also consistent with the results of a so-called Job plot[20] made from mixtures of **1** and **2** in $CD_2Cl_2$ under conditions of invariant total concentration as monitored by proton NMR spectroscopy. This latter approach, as shown in Figure 2, reveals that the relative G–C complex concentration approaches a maximum when the mole fraction of **1** is approximately 0.5, as is expected for the formation of a 1:1 complex between **1** and **2**. Further, the corresponding Job plot measurement carried out for a mixture of monomers **1** and **3** (Figure 2) shows a maximum when the mole fraction of **1** is *ca.* 0.67, a value that indicates a 2:1 stoichiometry between **1** and **3**. Unfortunately, the association constant for binding between **1** and **3** could not be determined experimentally. However, because each "side" of **3** should bind 1 equiv of **1** in an independent manner, we assume that association constant is in the same range as that observed for **1** and **2**.

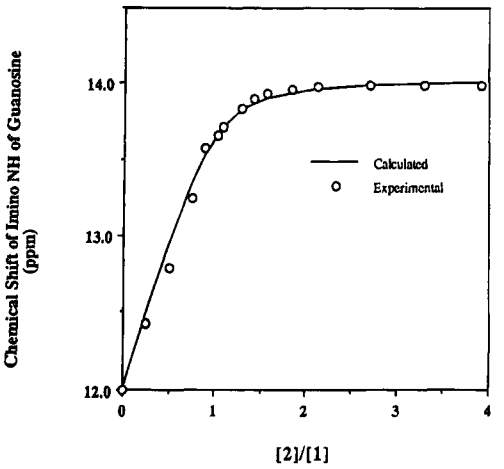


**Figure 1.** Experimental points and the computer generated curve corresponding to changes in the $^1H$ NMR spectra observed upon the addition of **2** to **1** in $CD_2Cl_2$ at room temperature. The chemical shift of the imino proton of the guanosine unit was monitored as a function of the ratio of **2** to **1**. The initial concentration of **1** was 1.0 mM. The derived binding constant was found to be $K = (2.2 \pm 0.2) \times 10^4\ M^{-1}$.

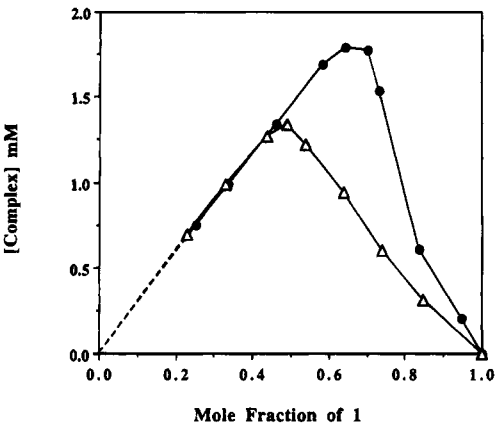


**Figure 2.** Job plot indicating the formation of a 1:1 supramolecular complex between **1** and **2** (△) and a 2:1 supramolecular complex between **1** and **3** (●). The total concentration was kept at 3.0 mM and the systems were monitored by $^1H$ NMR analysis (using the imino protons) in $CD_2Cl_2$ at room temperature. The maximum values of the complex concentration appear when the mole fractions of **1** are approximately 0.5 (△) and 0.67 (●) for the 1:1 and 2:1 complexes, respectively.

**Photophysical Properties of Nucleobase-Substituted Porphyrins.** The present approach to noncovalent energy-transfer ensemble development is predicated on the use of systems that contain nucleobase substituents appended directly (or almost directly) onto a porphyrin. While such attachment patterns are deemed essential for the formation of rigid, and hence mechanistically informative, donor–acceptor conjugates, it is nonethe-

(16) Saenger, W. In *Principles of Nucleic Acid Structure*; Springer-Verlag: New York, 1984; Chapter 6.
(17) Arnott, S.; Wilkins, M. H. F.; Hamilton, L. D.; Langridge, R. *J. Mol. Biol.* **1965**, *11*, 391.
(18) Witlock, B. J.; Witlock, H. W., Jr. *J. Am. Chem. Soc.* **1990**, *112*, 3910.
(19) (a) Pitha, J.; Jones, R. N.; Pithova, P. *Can. J. Chem.* **1966**, *44*, 1045. (b) Kyogoku, Y.; Lord, R. C.; Rich, A. *Biochim. Biophys. Acta* **1969**, *179*, 10. (c) Jorgensen, W. L.; Pranata, J. *J. Am. Chem. Soc.* **1990**, *112*, 2008. (d) Zimmerman, S. C.; Murray, T. J. *J. Am. Chem. Soc.* **1992**, *114*, 4010.
(20) (a) Connors, K. A. *Binding Constants. The Measurement of Molecular Complex Stability*; Wiley-Interscience: New York, 1987; p 22. (b) Blanda, M. T.; Horner, J. H.; Nencomb, M. *J. Org. Chem.* **1989**, *54*, 4626.

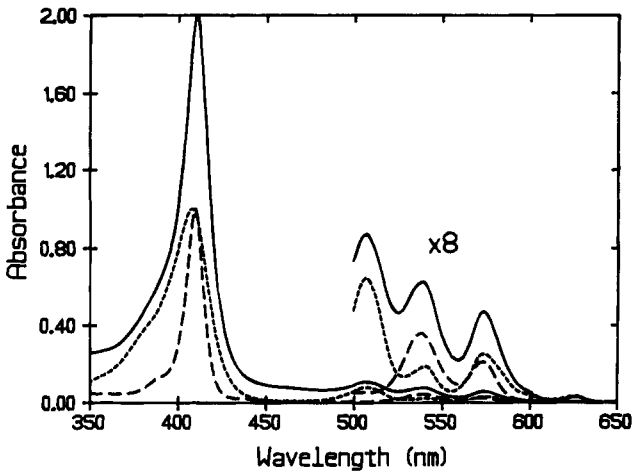


**Figure 3.** Absorption spectra recorded in $CH_2Cl_2$ at room temperature for compounds **1** (long dashed line) and **3** (short dashed line) and a 1:1 molar mixture (solid line) prepared from them.

**Table 1.** Photophysical Properties of Nucleobase-Substituted Porphyrins and Their Model Compounds as Measured in Dichloromethane Solution at 23 °C

| | $\lambda_{max}$ (nm) | | | | |
|---|---|---|---|---|---|
| porphyrins | Soret | *Q* | $\Phi_f$ | $\tau_s$ (ns) | $\tau_1$ ($\mu$s) |
| **1** | 411 | 539, 574 | 0.035 | 1.6 | 6.5 |
| **2** | 409 | 507, 541, 574, 626 | 0.090 | 12.9 | 9.8 |
| **3** | 410 | 508, 541, 574, 626 | 0.075 | 10.7 | 9.0 |
| **4** | 408 | 507, 541, 574, 625 | 0.065 | 9.3 | 9.6 |
| **5** | 410 | 539, 574 | 0.040 | 1.4 | 5.5 |

less necessary to test whether such substitution affects *in and of itself* the photophysical behavior of the individual chromophores. To this end, the optical properties of the nucleobase-substituted chromophores **1**–**3**, and several reference compounds, were studied using UV–visible and fluorescence spectroscopy.

A spectral comparison between **1** and its zinc diphenylporphyrin analogue **5**, and between **2** and **3** and the free-base form of this same control **4**, reveals that the relevant spectra are essentially superimposable. This leads us to suggest that the appended nucleobase does not perturb the spectra. Further, the absorption spectra recorded for the various supramolecular complexes formed between **1** and **2** and between **1** and **3** (Figure 3) indicate that the spectral features are basically the sum of those of the individual chromophores. Thus, at least as judged by these spectroscopic studies, there is no need to invoke any kind of direct interaction, such as $\pi$–$\pi$ stacking, between the chromophores.

Similar comparisons were made for fluorescence spectra recorded in dichloromethane, with excitation at 550 nm. The fluorescence spectra of the nucleobase-substituted porphyrins appear unaffected by the appended nucleobase moieties. This can be taken as an indication that the substituted nucleobases are electronically isolated from the porphyrins to which they are attached. Additional evidence was obtained from the measurements of the fluorescence quantum yields and lifetimes of these nucleobase-bearing porphyrins. As presented in Table 1, the fluorescence quantum yields and lifetimes for **1** and its model compound **5**, as well as those for **2**, **3**, and their model compound **4**, remain similar. Thus, the photophysical behavior of the nucleobase-bearing porphyrins **1**–**3** may be considered to be identical with that of the controls lacking such substituents.

**Singlet–Singlet Energy Transfer.** Time-resolved, single-photon counting fluorescence studies were made in air-equilibrated dichloromethane with excitation at 570 nm. The fluorescence lifetime of the zinc porphyrin component (at concentration of $\sim 10^{-5}$ M in $CH_2Cl_2$) was monitored at 600 nm where free-base porphyrins emit only extremely weakly. The fluorescence decay profile recorded for zinc guanosine–porphyrin **1** could be analyzed in terms of a single-exponential process with a lifetime ($\tau_s = 1.6 \pm 0.1$ ns) similar to that of the reference zinc porphyrin **5** ($\tau_s = 1.4$ ns) (Figure 4). This value was not substantially affected by the addition of up to 50 equiv of the nucleobase-free, unmetalated porphyrin **4**. However, when a cytidine-substituted free-base porphyrin (either **2** or **3**) was added to a $CH_2Cl_2$ solution of **1**, the decay profile became progressively dual-exponential (Figure 5) with a faster decaying component being seen in addition to the initially present slower one (Table 2). As was true in the case of analogous experiments carried out with the components of ensemble **I**,[14] the fractional amplitude of this shorter-lived component increased with increasing concentration of added **2** or **3**. However, the measured lifetimes remained essentially unaffected by changes in concentration.

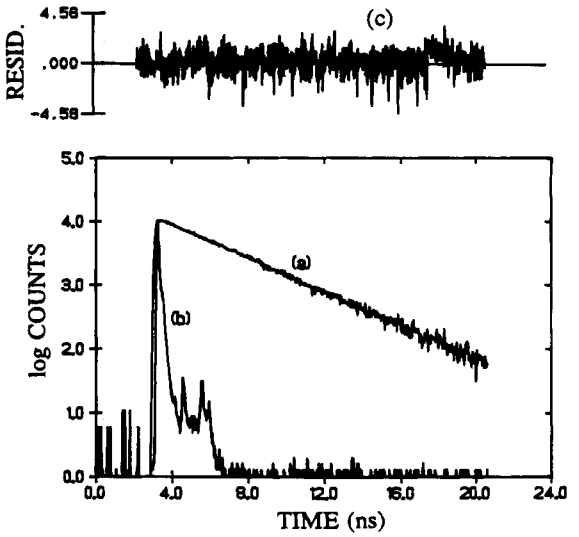


**Figure 4.** Time-correlated single-photon-counting decay profiles recorded in $CH_2Cl_2$ at room temperature for compound **1**: (a) experimental decay profile; (b) instrument response function; (c) residuals after fitting to one exponential with $\tau = 1.6$ ns ($\chi^2 = 1.07$). The excitation wavelength was 575 nm, while fluorescence detection was effected at 600 nm.

The longer lifetime ($\tau_1$) is assigned to that portion of the guanosine-containing zinc porphyrin that remains free in solution. The shorter-lived component ($\tau_2$), on the other hand, is considered to arise from that portion of the zinc guanosine-bearing porphyrin that is complexed to the free-base cytidine-containing porphyrin (i.e., that present in ensemble **II** or **III**). For this species, the shortened lifetime is considered to be reflective of zinc porphyrin-to-free-base porphyrin singlet–singlet energy transfer within the G–C base-paired ensembles. Operating on this assumption, rate constants for singlet-state energy transfer ($k_{ss}$) could be derived from the expression $k_{ss} = \{(1/\tau_2) - (1/\tau_1)\}$. The derived values are collected in Table 2 along with the corresponding quantum yields for energy transfer within the ensemble ($\Phi_s = k_{ss}/\{k_{ss} + (1/\tau_1)\}$).

Singlet-state energy transfer from zinc porphyrin to free-base porphyrin is believed to occur within the hydrogen-bonded complex. This contention is supported by several pieces of evidence: First, as would be expected for noncovalently constructed ensembles wherein the rate of intracomplex energy transfer is fast compared to that of dissociation of complex,[21] the derived rate constants (Table 2) were found to be indepen-

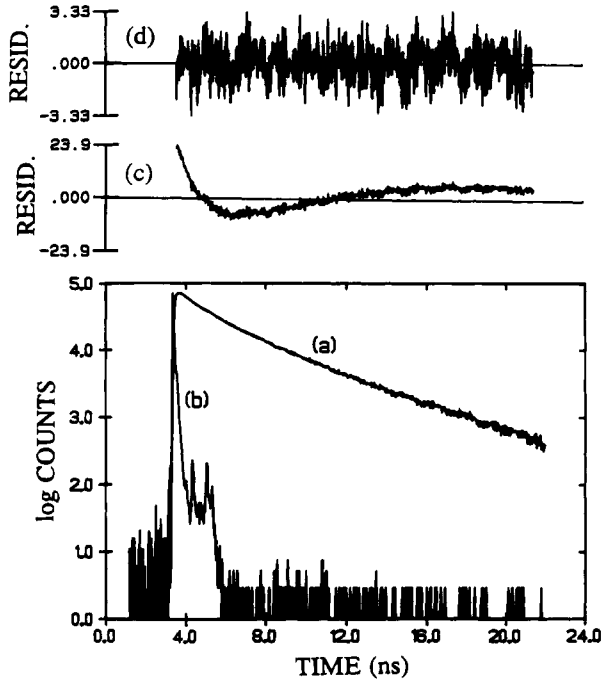


**Figure 5.** Time-correlated single-photon-counting decay profiles recorded in $CH_2Cl_2$ at room temperature for a mixture of **1** and **2** (ratio 4:1): (a) experimental decay profile; (b) instrument response function; (c) residuals after fitting to one exponential; (d) residuals after fitting to two exponentials with lifetimes of 1.6 ns and 0.70 ns ($\chi^2 = 1.12$). The excitation wavelength was 575 nm, while fluorescence detection was effected at 600 nm.

**Table 2.** Rate Constants ($k$) and Quantum Yields ($\Phi$) for Energy Transfer within Ensemble **II** and **III** Measured in Dichloromethane at 23 °C

| porphyrins | ratio **1**:**2** or **3** | $\tau_1$ (ns) | $\tau_2$ (ns) | $k_{ss}/10^8$ ($s^{-1}$) | $k_{obs}/10^6$ ($s^{-1}$) | $\Phi_s$ | $\Phi_t$ |
|---|---|---|---|---|---|---|---|
| **1** + **2** | 1:1 | 1.6 | 0.60 | 10.3 | 1.1 | 0.62 | 0.91 |
| | 1:3 | 1.6 | 0.70 | 8.1 | | 0.57 | |
| | 1:6 | 1.6 | 0.70 | 8.3 | | 0.57 | |
| | 4:1 | | | | 2.1 | | 0.95 |
| | 8:1 | | | | 3.9 | | 0.96 |
| **1** + **3** | 1:1 | 1.9 | 0.75 | 8.2 | 1.7 | 0.61 | 0.92 |
| | 4:1 | 1.9 | 0.70 | 9.4 | 2.0 | 0.64 | 0.93 |
| | 8:1 | 1.8 | 0.70 | 8.8 | 3.0 | 0.61 | 0.94 |

dent of the donor-to-acceptor ratio. Second, when a uridine-substituted porphyrin **6**[22] (analogous to **2**) was used in lieu of its cytidine analogue, as the putative energy acceptor, the fluorescence decay profile for the zinc porphyrin **1** could be analyzed satisfactorily in terms of a single exponential with a lifetime corresponding to that of the uncomplexed zinc porphyrin **1**. This latter case thus serves as an important control since the guanosine-substituted zinc porphyrin and the uridine-substituted free-base porphyrin are "mismatched" in terms of Watson–Crick base pairing. Finally, the Förster critical distance[23] for these particular couples is *ca.* 24 Å (*vide infra*), and the hydrogen-bonding interaction brings the two porphyrins to a center-to-center separation of *ca.* 22.5 Å.

(21) As a crude estimate the minimum lifetime of the hydrogen-bonded ensemble **II** can be estimated as being *ca.* 1 μs on the basis of $k_{diss} = k_{diff}/K$. Here, $K$ (=22 000 $M^{-1}$) is the association constant and $k_{diff}$ (=2 × $10^{10}$ $M^{-1}$ $s^{-1}$) is the diffusional controlled rate constant.

(22) The synthesis and full characterization data for this compound are reported elsewhere: Wang, B. Ph.D. Dissertation, The University of Texas at Austin, 1994.

(23) The Förster critical distance is defined as being the center-to-center distance between the two porphyrin subunits at which the rate of energy transfer equals the rate of inherent deactivation of the zinc porphyrin excited singlet state.

Further insight into the proposed intra-ensemble singlet–singlet energy transfer can be obtained from comparison with theory. Specifically, it is known that both dipole–dipole interaction (Förster)[24] and exchange (Dexter)[25] mechanisms are possible for singlet–singlet energy transfer. In both cases, the calculated rate constant is dependent on the overlap between the emission spectrum of the donor and the absorption spectrum of the acceptor. For Förster-type energy transfer, the overlap integral ($J_F$) was determined[24] to be (2.45 ± 0.05) × $10^{-14}$ mmol $cm^6$ for ensembles **II** and **III**:

$$J_F = \frac{\int F(\nu)\epsilon(\nu)\nu^{-4}\,d\nu}{\int F(\nu)\,d\nu} \quad (1)$$

where $F(\nu)$ is the fluorescence intensity at wavenumber $\nu$ (in $cm^{-1}$) and $\epsilon$ is the molar extinction coefficient (in $cm^{-1}$ $M^{-1}$) of the $Q_y$ absorption bands of the acceptor. Using these data along with the photophysical parameters obtained earlier, a value of 9.1 × $10^8$ $s^{-1}$ was derived for the energy-transfer rate constant ($k_{ss}$) within ensembles **II** and **III**. In both cases, calculations were made based on a center-to-center separation distance between the zinc porphyrin and the free-base porphyrin ($R_c$) of 22.5 Å and were made using the following equation:[24]

$$k_{ss} = \frac{(8.8 \times 10^{-25})K^2\Phi_f J_F}{n^4 \tau_s R_c^6} \quad (2)$$

Here, $K$ is an orientation factor describing the relative position of the donor and the acceptor ($K$ = 1)[26] and $n$ is the solvent refractive index. Based on the calculated rate constant, the corresponding energy-transfer efficiency ($\Phi_s$) could be estimated as being *ca.* 0.60 for ensembles **II** and **III**. Both the calculated rate ($k_{ss}$ = 9.1 × $10^8$ $s^{-1}$) and the resulting efficiency are thus consistent with the values obtained from experiment (Table 2). In fact, the excellent agreement between calculated and observed rates indicates that singlet energy transfer can be quantitatively explained in terms of Förster energy transfer. There is no need to allow for Dexter-type singlet energy transfer, and, in fact, calculations suggest to us that this process would be only a minor contributor to the overall energy-transfer pathway.[27] Here, it should be appreciated that the G–C hydrogen-bonding network only serves to tether together the chromophores and plays no role in facilitating the observed singlet–singlet energy-transfer process; this, of course, is as expected for a Förster-type process. Such a mechanism, however, is not operative in the case of triplet–triplet energy transfer, and, indeed, here the hydrogen-bonding tether appears to play a far more active, mediating role. This chemistry is described further below.

**Triplet–Triplet Energy Transfer.** The triplet excited-state properties of the individual nucleobase-bearing donor and acceptor, **1**, **2**, and **3**, as well as their hydrogen-bonded complexes, **II** and **III**, were studied by monitoring the transient

(24) Förster, T. *Discuss. Faraday Soc.* **1959**, *27*, 7.

(25) Dexter, D. L. *J. Chem. Phys.* **1953**, *21*, 836.

(26) The orientation factor is estimated to be (1.0 ± 0.2) on the basis of a side-by-side geometry with the transition dipoles arranged at 90°.

(27) The overlap integral for Dexter-type singlet energy transfer ($J_D$) was calculated to be 8.1 × $10^{-5}$ cm from spectral measurements. If the observed rate of energy transfer ($k_{ss}$ = 9 × $10^8$ $s^{-1}$) is due entirely to Dexter-type transfer, the electronic matrix coupling element ($V$) would have a value of 0.001 $cm^{-1}$ ($k_{ss} = 4\pi^2V^2J_D/h^2$[5]). Since this value is known to decrease exponentially with increasing separation distance ($V = V_0 \exp(-0.67R)$, where $R$ (=20 Å) is the edge-to-edge separation between the reactants estimated as the shortest through-bond distance, the electronic matrix coupling element at orbital contact would be *ca.* 600 $cm^{-1}$. This value seems unrealistically high and setting $V_0$ = 50 $cm^{-1}$ results in $k_{ss} \approx 3 \times 10^7$ $s^{-1}$.

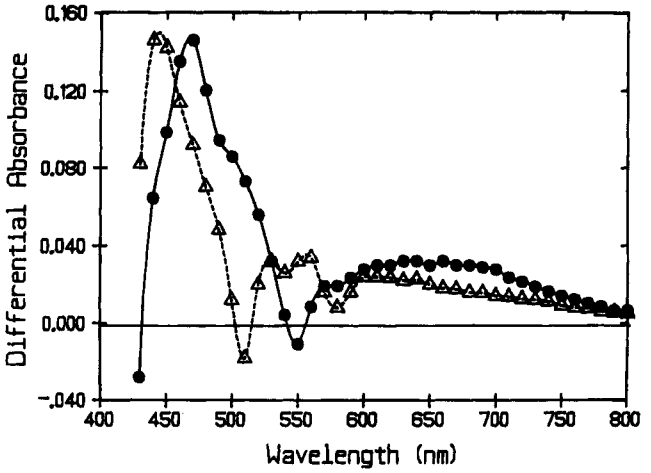


**Figure 6.** Triplet–triplet absorption spectra recorded in deoxygenated $CH_2Cl_2$ at room temperature for compounds **1** (●) and **2** (△). Spectra were recorded 100 ns after laser excitation at 532 nm.

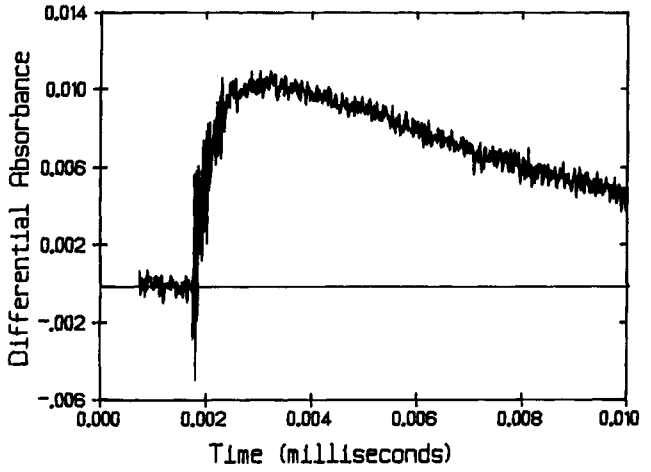


**Figure 7.** Kinetic profile recorded at 545 nm in deoxygenated $CH_2Cl_2$ at room temperature for the mixture of **1** and **2** (ratio 4:1) showing formation and subsequent decay of the free-base porphyrin triplet state.

absorption changes observed following excitation with a 10-ns laser pulse at 532 nm in deoxygenated dichloromethane at room temperature.[28] The absorption change was measured at 470 nm for the isolated porphyrins **1**–**5** and the derived triplet lifetimes are collected in Table 1. For ensembles **II** and **III**, the absorption change was measured at 545 nm since this is an isosbestic point for the zinc porphyrin chromophore and, therefore, allows selective monitoring of the free-base porphyrin triplet state (Figure 6). Under these conditions, the absorption change at 545 nm was observed to grow in after the laser pulse *via* first-order kinetics (Figure 7). This process is attributed to triplet energy transfer from a guanosine-substituted zinc porphyrin to a corresponding cytidine-substituted free-base porphyrin. For both ensembles, the observed first-order rate constant for appearance of the free-base porphyrin triplet ($k_{obs}$) was found to increase with increasing concentration of zinc porphyrin. This behavior is indicative of a diffusional energy-transfer process. Indeed, as can be seen from inspection of Figure 8, the diffusional reaction corresponds to a bimolecular

(28) It is interesting to note that the differential triplet absorption spectra and the triplet lifetimes measured for the various diphenyl octaalkyl porphyrins differ from those measured for the corresponding tetraphenylporphyrins or octaalkylporphyrins. This difference, which is more pronounced for the porphyrins containing a single nucleobase, is attributed to stereochemical disruption of the porphyrin ring arising from steric crowding around the substituted *meso* sites.

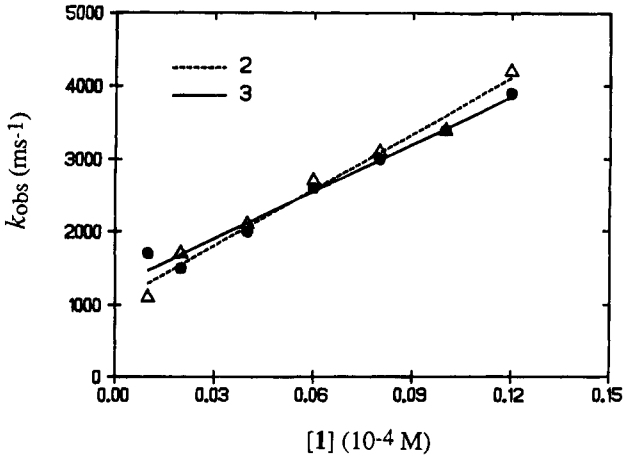


**Figure 8.** Plots showing the correlation of the observed rate constants ($k_{obs}$) for triplet-state energy transfer with the concentration of compound **1**. The free-base porphyrins used are compounds **2** (dashed line) and **3** (solid line).

triplet energy-transfer rate constant of *ca.* $2 \times 10^{10}$ $M^{-1}$ $s^{-1}$ for both ensembles. From the intercept to Figure 8, the *unimolecular* triplet energy-transfer rate constant, as extrapolated to zero concentration of zinc porphyrin, corresponds to a value of *ca.* $1 \times 10^6$ $s^{-1}$.[29] This latter process must refer to triplet energy transfer within a hydrogen-bonded ensemble and, as such, must conform to the Dexter mechanism.

In general, Dexter-type energy transfer requires orbital overlap of the donor and acceptor (so as to allow the requisite electron-exchange process to occur). In ensembles **II** and **III**, the zinc porphyrin and free-base porphyrin are separated by large center-to-center distances (*ca.* 22.5 Å). Further, both systems are such that direct contact between the chromophores is precluded (they are just too rigid). Thus, the observed intraensemble triplet–triplet energy-transfer process must proceed through bonds, as opposed to through-space. This, in turn, means that the hydrogen-bond bridges necessarily play a mediating role. This conclusion is consistent with ones made in the case of related noncovalent electron-transfer model systems[4a,5b] and is not unexpected given the ET-like nature of a Dexter-type energy-transfer process.

Diffusional triplet energy transfer was also observed to take place for the corresponding porphyrins not having nucleobase substituents. Again, the bimolecular rate constants were found to be *ca.* $2 \times 10^{10}$ $M^{-1}$ $s^{-1}$. Replacing **2** with a uridine-substituted free-base porphyrin **6** also resulted in bimolecular triplet energy transfer, but, unlike the situation found with ensembles **II** and **III**, there was no unimolecular process. This situation is entirely consistent with the unimolecular triplet energy-transfer reaction referring specifically to a hydrogen-bonded aggregate.[30]

(29) The observed rate constant for formation of the free-base porphyrin excited triplet state at any given concentration of zinc porphyrin ($k_{obs}$) is considered to be the sum of the rate constants for intra-ensemble (unimolecular) triplet energy transfer ($k_{tt}$) and for diffusional transfer ($k_{diff}$[**1**]). Analysis of Figure 8 gives $k_{tt} = 1.0 \pm 0.2 \times 10^6$ $s^{-1}$ and $k_{diff} = 2.6 \pm 0.2 \times 10^{10}$ $M^{-1}$ $s^{-1}$ for **II**; $k_{tt} = 1.2 \pm 0.2 \times 10^6$ $s^{-1}$ and $k_{diff} = 2.2 \pm 0.2 \times 10^{10}$ $M^{-1}$ $s^{-1}$ for **III**.

(30) It should be emphasized that the unimolecular triplet energy-transfer process is observed only for those couples that can form a three-point hydrogen bond. Identical experiments made with nucleobase-free porphyrins **4** and **5**, with mixtures of **1** and nucleobase-free nonmetalated porphyrin **4**, and with **1** and a uridine-derived free-base porphyrin **6**, all failed to show the unimolecular process. Furthermore, the amount of free-base porphyrin triplet state generated *via* intra-ensemble triplet energy transfer was observed to increase systematically with increasing concentrations of **1**.

## Concluding Remarks

The noncovalently assembled model systems described herein have been shown to represent an effective approach for studying photoinduced energy transfer. Singlet energy transfer occurs with a rate constant of *ca.* $9 \times 10^8$ $s^{-1}$ and with 60% efficiency, across a 22.5-Å center-to-center separation. Calculations based on both Förster and Dexter energy-transfer mechanisms suggest that the most probable singlet energy-transfer mechanism in the hydrogen-bonded systems is a Föster one. Triplet energy transfer from the guanosine−cytidine base-paired zinc porphyrin to the free-base porphyrin needs *ca.* 1 μs to cross the hydrogen-bonded network[21] in the absence of bimolecular processes, and occurs with almost quantitative efficiency. The longer triplet lifetime facilitates Dexter-type energy transfer, whereas this process is probably too slow to contribute significantly to the dynamics of the singlet state. However, Förster-type transfer is effective for singlet energy transfer, having a critical distance of *ca.* 24 Å for these particular chromophores. For optimal Förster transfer, therefore, the distance between the porphyrins in the hydrogen-bonded ensemble needs to be shortened. For example, in order to attain a quantum efficiency for singlet energy transfer of ~90%, the separation distance needs to be reduced by *ca.* 5 Å. This could easily be achieved in principle by, for instance, the removal of a single phenyl group in **II** or **III**.

The study presented here serves to demonstrate that hydrogen-bonding interactions can be used both to generate photoactive aggregates that are different from the traditional ones and to provide an effective pathway for mediating donor-to-acceptor triplet-energy transfer. This study thus stands as an important complement to our previous study of a photoactive hydrogen-bonded porphyrin−quinone system from which we concluded that hydrogen bonding could serve as an electron-transfer mediator.[5b] Further, and perhaps more importantly, this non-covalent approach to constructing energy-transfer model systems could also be applied to assemble higher-order arrays. Indeed, extensions of the present approach, wherein a combination of various noncovalent interactions are used as the means for self-assembly, are currently being actively pursued.

## Experimental Section

**General Information.** Proton nuclear magnetic resonance ($^1$H NMR) and carbon nuclear magnetic resonance ($^{13}$C NMR) spectra were recorded on a General Electrics QE-300 NMR spectrometer using either tetramethylsilane (TMS) or the residual peaks in deuterated solvents as internal standards. UV/visible spectra were obtained using either Beckman DU 7 or Hitachi U-3210 spectrophotometers. Fluorescence spectra were recorded with a Perkin-Elmer LS5 spectrofluorimeter. Chemical ionization mass spectrometric analyses (CI MS) were made using a Finnigan-MAT 4023 instrument. Fast atom bombardment mass spectra (FAB MS) were determined using a Finnigan-MAT TSQ instrument and a 3-nitrobenzyl alcohol matrix. High resolution mass spectra were obtained with a Bell and Howell 21-110B instrument. Elemental analyses were performed by Atlantic Microlab, Inc. (Norcross, GA).

Fluorescence lifetimes were measured using time-correlated, single-photon counting methods with a mode-locked, synchronously-pumped, cavity-dumped Rhodamine 6G dye laser serving as the excitation source. The excitation wavelength was 570 nm and the fluorescence was isolated from scattered laser light using a 590-nm glass cutoff filter and a high radiance monochromator. Emission was collected at 600 nm and analyzed after deconvolution of the instrument response function (fwhm = 60 ps). Transient absorption studies were made with a Q-switched, frequency-doubled Nd:YAG laser (pulse width 10 ns). All measurements were made in deoxygenated $CH_2Cl_2$.

**Materials.** Tetrahydrofuran (THF) was distilled from sodium and benzophenone. Pyridine was distilled from barium oxide. Methylene chloride was distilled from calcium hydride. Toluene was distilled from sodium. Anhydrous acetonitrile and *N,N*-dimethylformamide (DMF) were purchased from Aldrich Chemical Co. (Sure-Seal). The nucleic acid bases were brought from Sigma Chemical Co. All other solvents and reagents were of reagent grade quality and used as received. Thin layer chromatography (TLC) was performed on commercially prepared silica gel plates purchased from Whatman International, Inc. Column chromatography was performed using Merck silica gel 60 as the solid support.

**4-Tributylstannylbenzaldehyde (9).** A solution of 4-bromobenzaldehyde (2.78 g, 15.0 mmol) and bis(tributyltin) (17.4 g, 30.0 mmol) in toluene (100 mL) was bubbled with argon gas for 15 min before the introduction of the $Pd(PPh_3)_4$ catalyst (120 mg, 0.1 mmol). The resulting solution was heated at reflux under argon atmosphere for 18 h before being cooled and concentrated under reduced pressure. The resulting oil was purified on a silica gel column using first hexanes, and then 5% ethyl acetate in hexanes, as the eluents. This gave 4.0 g of product **9** as a colorless oil (66.9%): $^1$H NMR ($CDCl_3$) $\delta$ 0.89 (t, $J$ = 7.16 Hz, 12 H, $CH_2CH_2CH_2CH_3$), 1.13 (t, $J$ = 8.25 Hz, 6 H, $CH_2CH_2CH_2CH_3$), 1.34 (m, 6 H, $CH_2CH_2CH_2CH_3$), 1.54 (m, 6 H, $CH_2CH_2CH_2CH_3$), 7.67 (d, $J$ = 7.74 Hz, 2 H, Ph*H*), 7.77 (d, $J$ = 7.68 Hz, 2 H, Ph*H*), 9.99 (s, 1H, C*H*O); $^{13}$C NMR ($CDCl_3$) $\delta$ 9.7 ($CH_2CH_2CH_2CH_3$), 13.6 ($CH_2CH_2CH_2CH_3$), 27.3 ($CH_2CH_2CH_2CH_3$), 29.0 ($CH_2CH_2CH_2CH_3$), 128.4, 135.9, 136.9, and 152.5 (aromatic), 192.8 (*C*HO).

**2-Isobutyramido-8-bromo-9-(2,3,5-tri-*O*-isobutyryl-β-D-ribofuranosyl)purin-6-one (10).** To a suspension of 8-bromoguanosine (7.24 g, 20 mmol) in dry pyridine (200 mL) was added slowly isobutyryl chloride (34 mL, 240 mmol) at 0 °C. After the addition was complete, the mixture was stirred at 0 °C for 1 h and then poured into cold aqueous $NaHCO_3$ (5%, 100 mL). The resulting mixture was extracted with ethyl acetate (3 × 100 mL). The organic layer was then washed repeatedly with 100-mL portions of water and dried over anhydrous $Na_2SO_4$. After evaporative removal of the solvent, the resulting thick syrup was purified by column chromatography on silica gel using 50% ethyl acetate in hexanes as the eluent. This afforded 12.7 g of product **10** as a yellowish solid (98.9% yield): $^1$H NMR ($CDCl_3$) $\delta$ 1.09−1.31 (m, 24 H, $CH(CH_3)_2$), 2.50−2.80 (m, 4 H, $CH(CH_3)_2$), 4.46 (m, 2 H, H′5), 4.61 (q, 1 H, H′4), 5.90 (t, $J$ = 5.07 Hz, 1 H, H′3), 6.05 (d, $J$ = 4.40 Hz, 1 H, H′1), 6.15 (t, $J$ = 4.77 Hz, 1 H, H′2), 9.50 (s, 1 H, amide N*H*), and 12.26 (br s, 1 H, imino N*H*); $^{13}$C NMR ($CDCl_3$) $\delta$ 18.6 ($CH(CH_3)_2$), 18.7 ($CH(CH_3)_2$), 33.5 ($CH(CH_3)_2$), 33.6 ($CH(CH_3)_2$), 33.7 ($CH(CH_3)_2$), 36.2 ($CH(CH_3)_2$), 62.5 (C′5), 70.5 (C′2), 72.0 (C′3), 79.6 (C′4), 88.5 (C′1), 121.9 (C5), 123.9 (C8), 147.7 (C4), 148.6 (C2), 154.1 (C6), 175.3 ($COCH(CH_3)_2$), 175.9 ($COCH(CH_3)_2$), 177.4 ($COCH(CH_3)_2$), and 179.1 ($COCH(CH_3)_2$); mass spectrum (CI) *m/z* (relative intensity) 642 ($M^+$, 88), 644 ($M^+$ + 2, 100).

**4-[2-Isobutyramido-9-(2,3,5-tri-*O*-isobutyryl-β-D-ribofuranosyl)-purin-6-on-8-yl]benzaldehyde (11).** A solution of **10** (8.85 g, 13.8 mmol) and tributyltinbenzaldehyde (**9**) (6.67 g, 16.8 mmol) in toluene (150 mL) was purged with argon gas. Then, $Pd(PPh_3)_4$ (150 mg, 0.13 mmol) was added and the resulting solution heated at reflux under argon atmosphere for 38 h. It was then cooled, concentrated under reduced pressure, and then purified by silica gel column chromatography using 45% ethyl acetate in hexanes as the eluent. This gave product **11** (6.41 g, 69.7%) as a yellowish solid. There was also some starting material **10** recovered. $^1$H NMR ($CDCl_3$) $\delta$ 1.07−1.34 (m, 24 H, $CH(CH_3)_2$), 2.49−2.76 (m, 4 H, $CH(CH_3)_2$), 4.41 (m, 2 H, H′5), 4.63 (q, 1 H, H′4), 5.79 (t, 1 H, H′3), 6.27 (d + t, 2 H, H′1 and H′2), 8.02 (m, 4 H, Ph*H*), 9.25 (s, 1 H, amide N*H*), 10.1 (s, 1 H, C*H*O), 12.0 (br s, 1 H, N$^1$*H*); $^{13}$C NMR ($CDCl_3$) $\delta$ 18.6, 18.7, 18.8, and 18.9 ($CH(CH_3)_2$), 33.7, 33.8, 33.9, and 36.6 ($CH(CH_3)_2$), 62.2 (C′5), 70.7 (C′2), 72.6 (C′3), 78.9 (C′4), 87.6 (C′1), 115.1 (C5), 121.7 (C8), 129.9, 130.1, 134.3, and 137.0 (phenyl), 147.4 (C4), 148.5 (C2), 155.4 (C6), 175.5, 176.4, 177.4, and 178.7 ($OCCHMe_2$), 195.6 (PhCHO). Exact mass (CI) for $C_{33}H_{42}N_5O_{10}$: calcd, 668.293 17; found, 668.292 60.

**4-Benzamido-5-bromo-1-(2,3,5-tri-*O*-benzoyl-β-D-ribofuranosyl)-pyrimidin-2-one (13).** To a suspension of cytidine **12** (12.2 g, 50.0 mmol) in dry pyridine (500 mL) was added bromine (35 mL, 10% solution in $CCl_4$) at room temperature. Afer being stirred for 45 min, the ensuing clear solution was cooled to 0 °C in an ice-bath before benzoyl chloride (75 mL, 500 mmol) was added. After being stirred at room temperature for 2 h, the resulting solution was poured into

cold aqueous sodium bicarbonate (400 mL, 5% solution) and extracted with ethyl acetate (3 × 300 mL). The combined organic extracts were then washed with water and dried over anhydrous sodium sulfate. The solvent was then removed under reduced pressure using a rotary evaporator. The resulting residue was dissolved in dichloromethane, loaded onto silica gel column, and eluted with 35% ethyl acetate in hexanes. This afforded 31.9 g of product **13** as a white foam (86.4%): $^1$H NMR ($CDCl_3$) $\delta$ 4.20−4.89 (m, 3 H, H′4 and H′5), 5.77 (t, $J$ = 6.02 Hz, 1 H, H′2), 5.92 (q, $J$ = 5.16 Hz, 1 H, H′3), 6.45 (d, $J$ = 5.98 Hz, 1 H, H′1), 7.33−8.32 (m, 21 H, H6 and Ph*H*), and 13.13 (s, 1 H, N*H*); $^{13}$C NMR ($CDCl_3$) $\delta$ 63.8, 71.4, 74.0, 81.9, 87.7, 98.0, 128.2, 128.2, 128.5, 128.6, 128.9, 129.0, 129.1, 129.7, 129.9, 130.2, 133.0, 133.7, 133.8, 136.2, 139.3, 147.2, 155.3, 165.3, and 166.0; mass spectrum (CI) $m/z$ (relative intensity) 737 ($M^+$, 100). Exact mass for $C_{37}H_{28}N_3O_9Br$: calcd, 737.100 89; found, 737.102 10.

**4-Bromobenzyl *tert*-Butyldimethylsilyl Ether (15).** 4-Bromobenzyl alcohol (**14**) (9.40 g, 50.2 mmol), *tert*-butyldimethylsilyl chloride (9.80 g, 65.0 mmol), and imidazole (4.42 g, 65.0 mmol) were dissolved in anhydrous DMF (150 mL). This solution was allowed to stir at room temperature overnight and then poured into ice−water (600 mL). The resulting mixture was extracted with dichloromethane (2 × 250 mL). The organic layer was separated off and washed with saturated aqueous sodium bicarbonate (2 × 200 mL) and water (2 × 200 mL), then dried over anhydrous sodium sulfate. After evaporative removal of solvent, the oil-like residue was purified on a silica gel column using 15% ethyl acetate in hexanes as the eluent. This afforded product **15** as a colorless oil (14.8 g, 98% yield): $^1$H NMR ($CDCl_3$) $\delta$ 0.13 (s, 6 H, Si($CH_3$)$_2$-Bu$^t$), 0.97 (s, 9 H, SiMe$_2$C($CH_3$)$_3$), 4.71 (s, 2 H, benzylic $CH_2$), 7.21 (d, $J$ = 8.35 Hz, 2 H, Ph*H*), 7.48 (d, $J$ = 8.25 Hz, 2 H, Ph*H*); $^{13}$C NMR ($CDCl_3$) $\delta$ −5.3 (Si($CH_3$)$_2$Bu$^t$), 18.4 (SiMe$_2$*C*Me$_3$), 25.9 (SiMe$_2$C-($CH_3$)$_3$), 64.3 (benzylic $CH_2$O), 120.5, 127.7, 131.2, and 140.4 (aromatic).

**4-Tributylstannyl Benzyl *tert*-Butyldimethylsilyl Ether (16).** To a solution of **15** (14.0 g, 46.5 mmol) in THF was slowly added *n*-butyllithium (1.6 M in hexanes, 33 mL, 51.2 mmol) *via* a syringe under argon atmosphere with stirring at −78 °C. Tributyltin chloride (13.9 mL, 51.2 mmol) was introduced 30 min later *via* a syringe, and the resulting solution was allowed to stir at room temperature for 2 h. After the solvent was removed under reduced pressure, the resulting oil-like residue was purified using a silica gel column and hexanes as the eluent. The organotin compound **16** obtained this way is a colorless oil (12.8 g, 78.3% yield): $^1$H NMR ($CDCl_3$) $\delta$ 0.14, 0.15 (ss, 6 H, Si($CH_3$)$_2$Bu$^t$), 0.90−0.95 (m, 9 H, $CH_2CH_2CH_2CH_3$), 0.98, 0.99, 1.00 (sss, 9 H, SiMe$_2$C($CH_3$)$_3$), 1.06−1.12 (m, 6 H, $CH_2CH_2CH_2CH_3$), 1.31−1.41 (m, 6 H, $CH_2CH_2CH_2CH_3$), 1.54−1.64 (m, 6 H, $CH_2CH_2CH_2$-$CH_3$), 4.78 (s, 2 H, benzylic $CH_2$O), 7.32−7.49 (m, 4 H, Ph*H*); $^{13}$C NMR ($CDCl_3$) $\delta$ −5.3 (Si($CH_3$)$_2$Bu$^t$), 9.6 ($CH_2CH_2CH_2CH_3$), 13.7 ($CH_2$-$CH_2CH_2CH_3$), 18.4 (SiMe$_2$*C*Me$_3$)), 26.0 (SiMe$_2$C($CH_3$)$_3$), 27.4 ($CH_2CH_2$-$CH_2CH_3$), 29.1 ($CH_2CH_2CH_2CH_3$), 65.0 (benzylic $CH_2$O), 125.7, 126.0, 128.2, 136.3, and 141.1 (aromatic).

***tert*-Butyldimethylsilyl-4-[4-benzamido-1-(2,3,5-tri-*O*-benzoyl-β-D-ribofuranosyl)pyrimidin-4-on-5-yl]benzyl Alcohol (18).** A solution of **13** (11.07 g, 15.0 mmol), **16** (8.60 g, 16.9 mmol), and Pd(PPh$_3$)$_4$ (100 mg, 0.06 mmol) in toluene (250 mL) was flushed with argon gas for 15 min before being brought to refluxing for 40 h under an argon atmosphere. The solvent was removed under reduced pressure, and the resulting residues were loaded on the top of a silica gel column and then eluted with 35% ethyl acetate in hexanes. This yielded *ca.* 10 g of yellowish solid consisting of **13** and **17**. Without further purification, this mixture was subjected to next desilylation reaction by treating with tetrabutylammonium fluoride (TBAF) (1.0 M solution in THF, 20 mL, 20.0 mmol) in dry THF (150 mL) at room temperature for 20 h, at which point TLC analysis indicated the completion of reaction. The reaction was quenched by adding water (100 mL). The resulting solution was then extracted with chloroform (3 × 150 mL). The combined organic extracts were washed with water, dried over anhydrous sodium sulfate, and concentrated using a rotary evaporator. Purification was performed using column chromatography (silica gel, 40% EtOAc in hexanes) and provided product **18** as a yellowish solid (6.40 g, 55.6% overall yield for the coupling and desilylation reactions): $^1$H NMR ($CDCl_3$) $\delta$ 4.72 (s, 2 H, benzylic $CH_2$O), 4.74−4.86 (m, 4 H, benzylic O*H*, H′4, and H′5), 5.93−6.03 (m, 2 H, H′2 and H′3), 6.52 (d, $J$ = 5.73 Hz, 1 H, H′1), 7.74 (s, 1 H, H6), 7.29−8.18 (m, 24 H, Ph*H*), 7.99 (s, 1 H, amide N*H*); $^{13}$C NMR ($CDCl_3$) $\delta$ 63.8, 64.4, 71.3, 73.7, 80.6, 88.0, 117.0, 126.3, 127.9, 128.1, 128.3, 128.7, 129.1, 129.3, 129.5, 129.7, 129.8, 131.1, 132.4, 133.3, 136.5, 137.9, 140.8, 147.4, 157.8, 165.2, 165.8; mass spectrum (CI) $m/z$ (relative intensity) 765 ($M^+$, 55).

**4-Benzamido-1-(2,3,5-tri-*O*-benzoyl-β-D-ribofuranosyl)pyrimidin-4-on-5-yl]benzaldehyde (19).** A 100-mL round-bottom flask was charged with **18** (1.53 g, 2.0 mmol), pyridinium dichromate (PDC) (1.88 g, 5.0 mmol), and freshly distilled dichloromethane (90 mL). The resulting mixture was then stirred at room temperature for 3 h. At this point TLC analysis indicated a complete disappearance of **18**. The reaction mixture was then poured into a brine solution and extracted with dichloromethane (3 × 50 mL). The combined organic extracts were washed repeatedly with water and dried over anhydrous sodium sulfate. The drying reagent was removed by filtering through a Celite pad. The solvent was removed under reduced pressure and the product purified by column chromatography (silica gel, 40% ethyl acetate in hexanes, eluent) to yield 1.21 g of **19** as a white solid (79.3%): $^1$H NMR ($CDCl_3$) $\delta$ 4.55−4.60 (dd, 1 H, H′5), 4.68 (m, 1 H, H′4), 4.74−4.79 (dd, 1 H, H′5), 5.78 (t, $J$ = 6.06 Hz, 1 H, H′2), 5.87 (t, $J$ = 3.62 Hz, 1 H, H′3), 6.46 (d, $J$ = 6.34 Hz, 1 H, H′1), 7.66 (s, 1 H, H6), 7.45−7.99 (m, 25 H, Ph*H*, and amide N*H*), 9.87 (C*H*O); $^{13}$C NMR ($CDCl_3$) $\delta$ 64.0, 71.4, 73.8, 81.0, 87.4, 116.3, 128.1, 128.4, 128.6, 129.1, 129.3, 129.5, 129.7, 129.8, 131.2, 132.7, 133.5, 133.7, 136.4, 138.4, 147.2, 157.3, 165.3, 165.8, 191.6; mass spectrum (CI) $m/z$ (relative intensity) 763 ($M^+$, 100). Exact mass for $C_{44}H_{44}N_3O_{10}$ ($M^+$ + H): calcd, 764.224 42; found, 764.222 10.

**1-[2-Isobutyramido-9-(2,3,5-tri-*O*-isobutyryl-β-D-ribofuranosyl)-purin-6-on-8-yl]-4-[5-(3,7,13,17-tetramethyl-2,8,12,18-tetrabutyl-15-phenyl)porphyrinyl]benzene (21).** A solution of **11** (1.50 g, 2.25 mmol), bis(4-methyl-3-butyl-2-pyrryl)methane (**20**) (1.29 g, 4.51 mmol), and benzaldehyde (0.239 g, 2.25 mmol) in freshly distilled dichloromethane (90 mL) was purged with argon gas for 15 min before trifluoroacetic acid (200 μL) was added *via* a syringe. The reaction vessel was covered with aluminum foil and the reaction was allowed to stir for 4 h. After being neutralized by the addition of sodium acetate (0.5 g) and oxidized using *p*-chloranil (1.6 g, 6.5 mmol), the reaction mixture was allowed to stir for an additional 6 h. The solvent was removed *in vacuo* and the resulting residue purified by column chromatography on silica gel (10% acetonitrile in $CH_2Cl_2$, eluent) to afford 980 mg of **21** (27%). Also obtained were (3,7,13,17-tetramethyl-2,8,12,18-tetrabutyl-5,15-diphenyl)porphyrin (**4**, 760 mg, 25%) and [5,-15-bis[4-(2-isobutyramido-9-(2,3,5-tri-*O*-butyryl-β-D-ribofuranosyl)-purin-6-on-8-yl)phenyl]-3,7,13,17-tetramethyl-2,8,12,18-tetrabutyl]-porphyrin (**23**, 533 mg, 33%). For **21**: $^1$H NMR ($CDCl_3$) $\delta$ −2.30 (br s, 2 H, internal N*H*), 1.09−1.17 (m, 18 H, CH($CH_3$)$_2$ on the sugar ring), 1.28 (t, 12 H, $CH_2CH_2CH_2CH_3$), 1.39 (m, 6 H, CH($CH_3$)$_2$N), 1.75 (m, 8 H, $CH_2CH_2CH_2CH_3$), 2.18 (m, 8 H, $CH_2CH_2CH_2CH_3$), 2.46 (s, 6 H, 3,7-$CH_3$), 2.55 (s, 6 H, 13,17-$CH_3$), 2.64−3.75 (m, 4 H, C*H*($CH_3$)$_2$), 3.95 (m, 8 H, $CH_2CH_2CH_2CH_3$), 4.60 (m, 2 H, H′5), 4.78 (m, 1 H, H′4), 6.34−6.43 (m, 3 H, H′3, H′2, and H′1), 7.71−8.26 (m, 9 H, Ph*H*), 9.36 (s, 1 H, amide N*H*), 10.24 (s, 2 H, meso-*H*), 12.20 (s, 1 H, imino N$^1$*H*); $^{13}$C NMR ($CDCl_3$) $\delta$ 13.9, 14.0, 14.2, 14.6, 14.8, 18.8, 23.1, 23.1, 23.3, 25.6, 26.2, 26.4, 33.9, 35.4, 36.6, 62.5, 71.0, 72.7, 79.2, 88.0, 97.0, 116.3, 116.4, 118.3, 118.9, 121.7, 127.6, 127.8, 128.3, 128.7, 128.8, 129.0, 142.0, 143.0, 143.3, 144.6, 145.2, 147.3, 148.6, 150.2, 155.6, 175.4, 176.3, 177.6, and 178.8; mass spectrum (FAB) $m/z$ (relative intensity) 1305 ($M^+$, 33). Exact mass (FAB) for $C_{78}H_{97}N_8O_9$: calcd, 1303.740 93; found, 1303.739 84.

**Zinc(II) Complex of 1-[2-Amino-7-(2,3,5-tri-*O*-*tert*-butyldimethylsilyl-β-D-ribofuranosyl)purin-6-on-8-yl]-4-[5-(3,7,13,17-tetramethyl-2,8,12,18-tetrabutyl-15-phenyl)porphyrinyl]benzene (1).** Compound **21** (256 mg, 0.20 mmol) was dissolved in 50 mL of saturated methanolic ammonia (saturated at −10 °C) and allowed to stand at room temperature for 36 h. The solvents were then removed *in vacuo* and the residue was dissolved in dichloromethane (25 mL), washed with water (3 × 25 mL), dried over anhydrous sodium sulfate, and evaporated to dryness. After being kept under vacuum at 50 °C for 5 h, the resulting material, along with *tert*-butyldimethylsilyl chloride (TBDMS-Cl) (180 mg, 1.2 mmol) and imidazole (81 mg, 1.2 mmol), was dissolved in anhydrous DMF (10 mL) at 0 °C with the aid of a

magnetic stirrer. The stirring was continued at room temperature overnight. The resulting mixture was then poured into crushed ice while stirring with a glass rod. The precipitate so obtained was then collected by filtration and dissolved in dichloromethane (25 mL). The resulting solution was washed with saturated aqueous sodium bicarbonate (2 × 50 mL) and water (2 × 50 mL) before being dried over anhydrous $Na_2SO_4$. After evaporative removal of solvent, the resulting residue (**22**) was dissolved in a saturated methanolic solution of zinc acetate (50 mL) and then heated at reflux for 30 min before being partitioned between dichloromethane and water (1:1 v/v, 50 mL). The organic layer was washed with water (2 × 25 mL), dried over anhydrous $Na_2SO_4$, and concentrated under reduced pressure. The desired product **1** was then isolated (silica gel column, 2% MeOH in $CHCl_3$, eluent) as a purple-red solid in 50% overall yield: $^1$H NMR ($CDCl_3$) $\delta$ −0.06−0.20 (m, 18 H, $Si(CH_3)_2Bu^t$), 0.90−0.93 (m, 27 H, $SiMe_2C(CH_3)_3$), 1.14 (m, 12 H, $CH_2CH_2CH_2CH_3$), 1.79 (m, 8 H, $CH_2CH_2CH_2CH_3$), 2.21 (m, $CH_2CH_2CH_2CH_3$), 2.46 and 2.58 (ss, 12 H, 3,7,13,17-$CH_3$), 3.62 (m, 1 H, H′2), 3.99 (m, 8 H, $CH_2CH_2CH_2CH_3$), 4.21 (m, 2 H, H′5), 4.55 (q, $J$ = 3.54 Hz, 1 H, H′4), 5.84 (t, $J$ = 4.45 Hz, 1 H, H′3), 6.08 (br s, 2 H, $NH_2$), 6.41 (d, $J$ = 6.67 Hz, 1 H, H′1), 7.78 (m, 3 H, 5- and 15-phenyl-H), 8.10 (d, $J$ = 6.59 Hz, 2 H, 5-phenyl-H), 8.27 (s, 3 H, 15-phenyl-H), 10.20 (s, 2 H, meso-H), and 12.43 (br s, 1 H, imino N$^1$H); mass spectrum (FAB) $m/z$ (relative intensity) 1431 ($M^+$ + 1, 76). Exact mass for $C_{80}H_{113}N_9O_5Si_3Zn$: calcd, 1427.746 399; found, 1427.746 46. Anal. Calcd for $C_{80}H_{113}N_9O_5Si_3Zn$: C, 67.17; H, 7.96; N, 8.81. Found: C, 66.91; H, 7.99; N, 8.74.

**4-[4-Benzamido-1-(2,3,5-tri-*O*-benzoyl-β-D-ribofuranosyl)pyrimidin-2-on-5-yl]-1-[5-(3,7,13,17-tetramethyl-2,8,12,18-tetrabutyl-15-phenyl)porphyrinyl]benzene (24) and 4-Bis[4-benzamido-1-(2,3,5-tri-*O*-benzoyl-β-D-ribofuranosyl)pyrimidin-2-on-5-yl]-1-[5-(3,7,13,17-tetramethyl-2,8,12,18-tetrabutyl)porphyrinyl]benzene (25).** A solution of **19** (0.60 g, 0.78 mmol) and benzaldehyde (80 μL, 0.78 mmol) in freshly distilled dichloromethane (80 mL) was bubbled with argon gas for 15 min before **20** (0.45 g, 1.57 mmol) was added. The reaction vessel was shielded from the ambient light with aluminum foil. To this solution was added trifluoroacetic acid (15 μL) *via* a syringe. The mixture was then stirred at room temperature under argon atmosphere for 7 h before being neutralized by the addition of a small amount of sodium acetate powder. One hour later, *p*-chloranil (0.20 g) was introduced to the solution, and the resulting oxidation reaction was allowed to proceed at room temperature overnight. The reaction solution was then concentrated and loaded onto the top of a silica gel column. Eluting first with chloroform gave 5,15-diphenylporphyrin **4** (126 mg, 43%). Using 2% acetonitrile in dichloromethane then yielded the monosubstituted cytidine porphyrin **24** (360 mg, 33%). Finally eluting with 3% methanol in chloroform furnished the disubstituted cytidine porphyrin **25** (117 mg, 15%). For **24**: $^1$H NMR ($CDCl_3$) $\delta$ 1.13−1.19 (m, 12 H, $CH_2CH_2CH_2CH_3$), 1.81 (m, 8 H, $CH_2CH_2CH_2CH_3$), 2.21 (m, 8 H, $CH_2CH_2CH_2CH_3$), 2.53, 2.55 (ss, 12 H, 3,7,13,17-$CH_3$), 4.04 (m, 8 H, $CH_2CH_2CH_2CH_3$), 4.87−5.02 (m, 3 H, H′4 and H′5), 6.13 (m, 2H, H′2 and H′3), 6.73 (d, 1 H, H′1), 7.37−8.40 (m, 26 H, H6, PhH and amide N), 10.31 (s, 2 H, meso-H); mass spectrum (FAB) $m/z$ (relative intensity) 1401 ($M^+$, 27). For **25**: $^1$H NMR ($CDCl_3$) $\delta$ −1.94 (br s, 2 H, internal NH), 1.15 (t, $J$ = 7.32 Hz, 12 H, $CH_2CH_2CH_2CH_3$), 1.83 (sextet, $J$ = 7.34 Hz, 8 H, $CH_2CH_2CH_2CH_3$), 2.25 (quintet, $J$ = 7.46 Hz, 8 H, $CH_2CH_2CH_2CH_3$), 2.54 (s, 12 H, 3,7,13,17-$CH_3$), 4.06 (t, $J$ = 7.28 Hz, 8 H, $CH_2CH_2CH_2CH_3$), 4.80−5.00 (m, 3 H, H′4 and H′5), 6.08 (m, 2 H, H′2 and H′3), 6.71 (d, $J$ = 5.49 Hz, 1 H, H′1), 7.38−8.38 (m, 26 H, H6, PhH and amide NH), 10.33 (s, 2 H, meso-H); mass spectrum (FAB) $m/z$ (relative intensity) 2059 ($M^+$ + 1, 40).

**4-[4-Amino-1-(2,3,5-tri-*O*-*tert*-butyldimethylsilyl-β-D-ribofuranosyl)pyrimidin-2-on-5-yl]-1-[5-(3,7,13,17-tetramethyl-2,8,12,18-tetrabutyl-15-phenyl)porphyrinyl]benzene (2) and 4-Bis[4-amino-1-(2,3,5-tri-*O*-*tert*-butyldimethylsilyl-β-D-ribofuranosyl)pyrimidin-2-on-5-yl]-1-[5-(3,7,13,17-tetramethyl-2,8,12,18-tetrabutyl)porphyrinyl]benzene (3).** Compounds **2** and **3** were prepared from **24** and **25**, respectively, using the same procedures used to prepare compounds **22**. For **2**, a 60% yield was obtained (silica gel column, 1% MeOH in $CHCl_3$, eluent): $^1$H NMR ($CDCl_3$) $\delta$ −2.28 (br s, 2 H, internal N-H), 0.022−0.37 (m, 18 H, $Si(CH_3)_2C(CH_3)_3$), 1.03 (m, 27 H, $Si(CH_3)_2C(CH_3)_3$), 1.17 (m, 12 H, $CH_2CH_2CH_2CH_3$), 1.82 (m, 8 H, $CH_2CH_2CH_2CH_3$), 2.25 (m, 8 H, $CH_2CH_2CH_2CH_3$), 2.54, 2.59 (ss, 12 H, 3,7,13,17-$CH_3$), 3.89−3.93 (m, 2 H, H′5), 4.05 (m, 8 H, $CH_2CH_2CH_2CH_3$), 4.24 (m, 2 H, H′3, H′4), 4.48 (t, 1 H, H′2), 5.75 (br s, 2 H, $NH_2$), 6.41 (d, 1 H, H′1), 7.78−8.22 (m, 9 H, PhH), 7.92 (s, 1 H, H6), 10.32 (s, 2 H, meso-H); $^{13}$C NMR ($CDCl_3$) $\delta$ −5.3, −5.0, −4.6, −4.4, −4.3, 14.2, 14.6, 15.2, 18.2, 18.6, 23.3, 25.7, 25.9, 26.2, 26.5, 35.5, 63.6, 72.5, 75.6, 77.2, 85.6, 88.6, 97.1, 109.0, 116.4, 118.3, 127.6, 128.1, 128.3, 132.9, 134.1, 135.5, 136.4, 139.9, 141.4, 141.6, 142.9, 143.3, 143.5, 144.9, 145.3, 155.7, 164.2; mass spectrum (FAB) $m/z$ (relative intensity) 1327 ($M^+$, 100). Exact mass for $C_{79}H_{116}N_7O_5Si_3$: ($M^+$ + H) calcd, 1326.834 58; found, 1326.838 54. For **3**, a 40% yield was obtained: $^1$H NMR ($CDCl_3$) $\delta$ −2.30 (br s, 2 H, internal N-H), 0.03−0.32 (m, 36 H, $Si(CH_3)_2C(CH_3)_3$), 0.92−1.03 (m, 54 H, $Si(CH_3)_2C(CH_3)_3$), 1.10−1.16 (m, 12 H, $CH_2CH_2CH_2CH_3$), 1.80 (m, 8 H, $CH_2CH_2CH_2CH_3$), 2.21 (m, 8 H, $CH_2CH_2CH_2CH_3$), 2.43, 2.58 (ss, 12 H, 3,7,13,17-$CH_3$), 3.89−3.93 (m, 2 H, H′5), 4.01 (m, 8 H, $CH_2CH_2CH_2CH_3$), 4.24 (m, 2 H, H′3, H′4), 4.48 (t, 1 H, H′2), 5.72 (br s, 2 H, $NH_2$), 6.41 (d, 1 H, H′1), 7.78−8.22 (m, 8 H, PhH), 7.92 (ss, 2 H, H6), 10.30 (s, 2 H, meso-H); mass spectrum (FAB) $m/z$ (relative intensity) 1911 ($M^+$, 19). Exact mass for $C_{106}H_{169}N_{10}O_{10}Si_6$: ($M^+$ + H) calcd, 1910.163 89; found, 1910.158 36.

**Determination of Binding Constant by NMR.** To 1000 μL of a 1.0 mM solution of **1** in $CD_2Cl_2$ were added sequentially aliquots of a 25.9 mM solution of **2** in $CD_2Cl_2$. The changes in the chemical shift values of the guanine imino protons were recorded as a function of the latter concentration. Data reduction was then effected using the nonlinear least-square NMR curve fitting of Whitlock[18] as described in greater detail elsewhere.[31]

**Determination of Stoichiometry of the Complexations between 1 and 2 or 1 and 3 by NMR.** To 700 μL of a 3.0 mM solution of **1** in $CD_2Cl_2$ were added sequentially aliquots of a 3.0 mM solution of **2** or **3** in $CD_2Cl_2$ while at each juncture equal portions of the mixture were removed. By this means, the mole fraction of **1** was varied while the total concentration of **1** and **2** or **1** and **3** was held constant. The corresponding chemical shift changes for the guanine imino in **1** were then recorded and standard data manipulations carried out to derive the complex concentration.[20] Job plots were then generated by plotting the mole fraction of **1** vs the concentration of the complex.

**Acknowledgment.** This work was supported by the R. A. Welch Foundation (F-1018), the National Institutes of Health (GM-41657 to J.L.S.), and the National Science Foundation (CHE 9102657 to A.H.). The Center for Fast Kinetics Research is supported by the University of Texas at Austin.

JA942582O

(31) Sessler, J. L.; Magda, D. J.; Furuta, H. *J. Org. Chem.* **1992**, *57*, 818.